



HAL
open science

Chronology reconstruction for the disturbed bottom section of the GISP2 and the GRIP ice cores: Implications for Termination II in Greenland

Makoto Suwa, Joseph C von Fischer, Michael Bender, Amaelle Landais,
Edward J Brook

► **To cite this version:**

Makoto Suwa, Joseph C von Fischer, Michael Bender, Amaelle Landais, Edward J Brook. Chronology reconstruction for the disturbed bottom section of the GISP2 and the GRIP ice cores: Implications for Termination II in Greenland. *Journal of Geophysical Research*, 2006, 111 (D2), 10.1029/2005jd006032 . hal-03189900

HAL Id: hal-03189900

<https://hal.science/hal-03189900>

Submitted on 5 Apr 2021

HAL is a multi-disciplinary open access archive for the deposit and dissemination of scientific research documents, whether they are published or not. The documents may come from teaching and research institutions in France or abroad, or from public or private research centers.

L'archive ouverte pluridisciplinaire **HAL**, est destinée au dépôt et à la diffusion de documents scientifiques de niveau recherche, publiés ou non, émanant des établissements d'enseignement et de recherche français ou étrangers, des laboratoires publics ou privés.

Chronology reconstruction for the disturbed bottom section of the GISP2 and the GRIP ice cores: Implications for Termination II in Greenland

Makoto Suwa, Joseph C. von Fischer,¹ and Michael L. Bender

Department of Geosciences, Princeton University, Princeton, New Jersey, USA

Amaelle Landais²

Institut Pierre-Simon Laplace/Laboratoire des Sciences du Climat et de l'Environnement, CEA-CNRS, Gif sur Yvette, France

Edward J. Brook

Department of Geosciences, Oregon State University, Wilkinson Hall, Corvallis, Oregon, USA

Received 31 March 2005; revised 24 August 2005; accepted 28 October 2005; published 17 January 2006.

[1] We have reconstructed chronology for the disturbed bottom parts of the GRIP and GISP2 ice cores using the combined paleoatmospheric records of CH₄ concentration and $\delta^{18}\text{O}_{\text{atm}}$ in the trapped gases. Our reconstructed ages for basal ice samples are based on comparison of published measurements of CH₄ and $\delta^{18}\text{O}_{\text{atm}}$ from the disturbed section of the GRIP and GISP2 cores with the same properties in the Vostok ice core. NGRIP $\delta^{18}\text{O}_{\text{ice}}$ values are also used to constrain the chronology during the end of marine isotope stage 5e. For each sample, we assign an age that represents the unique or most probable time of gas trapping, given its gas composition. Of 157 samples with CH₄ and $\delta^{18}\text{O}_{\text{atm}}$ data, 10 give unique ages. Twenty-five newly measured values of the triple isotope composition of O₂ from the disturbed section of the GISP2 core add a third time-dependent gas property that agrees with our reconstruction. Our reconstruction supports earlier conclusions of Landais et al. (2003) that the disturbed section primarily includes ice from the last interglacial (MIS 5e) and the penultimate glacial period (MIS 6). The oldest ice in the basal layer of GISP2 and GRIP has an age ≥ 237 ka. The climate history we derive suggests that the last interglacial at Summit, Greenland, around 127 ka was slightly warmer than the current interglacial period. Reduction of various ion concentrations in ice and thickening of the ice sheet during Termination II was similar to that in Termination I.

Citation: Suwa, M., J. C. von Fischer, M. L. Bender, A. Landais, and E. J. Brook (2006), Chronology reconstruction for the disturbed bottom section of the GISP2 and the GRIP ice cores: Implications for Termination II in Greenland, *J. Geophys. Res.*, *111*, D02101, doi:10.1029/2005JD006032.

1. Introduction

[2] Two ice cores drilled by the Greenland Ice Core Project (GRIP) and the Greenland Ice Sheet Project Two (GISP2) from Summit, Greenland record variations in Greenland climate during the past ~ 100 ka [e.g., Dansgaard et al., 1993; GRIP Project Members, 1993; Grootes et al., 1993; Chappellaz et al., 1993; Brook et al., 1996]. Temperature reconstructions based on $\delta^{18}\text{O}$ of ice ($\delta^{18}\text{O}_{\text{ice}}$) from these cores show remarkably good agreement until 100–105 ka [Grootes et al., 1993]. In older samples, differences

in $\delta^{18}\text{O}_{\text{ice}}$ between the two cores have led to the conclusion that at least one is stratigraphically disturbed [Grootes et al., 1993]. Bender et al. [1994a] and Chappellaz et al. [1997a] concluded that both cores have a disturbed bottom section by showing that the records of CH₄ concentration and $\delta^{18}\text{O}$ of paleoatmospheric O₂ ($\delta^{18}\text{O}_{\text{atm}}$, gravitationally corrected) versus depth in the trapped gases of the Greenland cores are significantly different from those of the Vostok core. The new core drilled by the North Greenland Ice Core Project (NGRIP) [North Greenland Ice Core Project Members, 2004] extends the record of Greenland climate back to ~ 123 ka. The climate history can currently only be extended by ordering of the ice in the disturbed sections of GISP2 and GRIP. We note that the bottom of the Camp Century ice core has $\delta^{18}\text{O}_{\text{ice}}$ heavier than Holocene values and this may indicate ice from the last interglacial [Johnsen et al., 1972]. A chronology for the bottom part of the Camp Century ice

¹Now at Department of Biology, Colorado State University, Fort Collins, Colorado, USA.

²Now at Institute of Earth Sciences, Hebrew University of Jerusalem, Jerusalem, Israel.

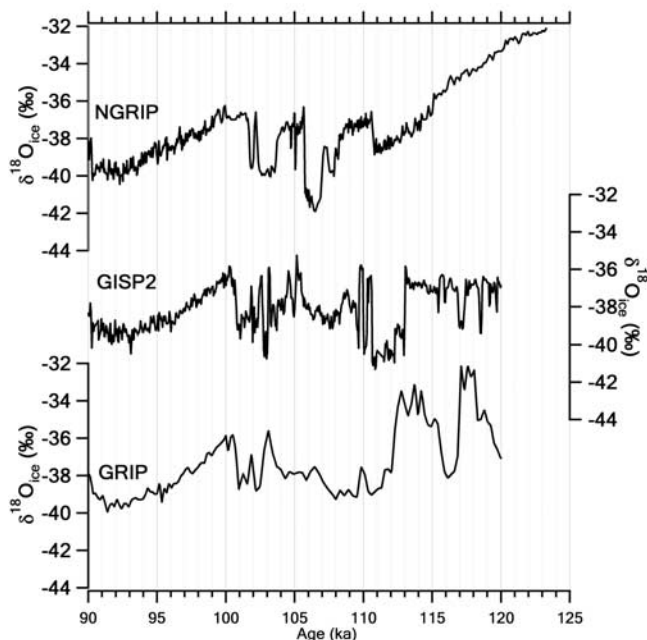


Figure 1. Comparison of $\delta^{18}\text{O}_{\text{ice}}$ of GISP2 [Grootes *et al.*, 1993], GRIP [Dansgaard *et al.*, 1993] and NGRIP [North Greenland Ice Core Project Members, 2004] ice cores between 125 ka and 90 ka. GISP2, GRIP and NGRIP curves are plotted on the GISP2 timescale [Meese *et al.*, 1994; Sowers *et al.*, 1993] until 101 ka. This chronology is extrapolated for a period prior to 101 ka as if there had been no basal mixing in GISP2 and GRIP. NGRIP chronology prior to 101 ka is from Landais *et al.* [2006].

core is also uncertain, however, no CH_4 and $\delta^{18}\text{O}_{\text{atm}}$ records are available.

[3] Landais *et al.* [2004] demonstrated that the previously inferred dramatic cooling of the 5e1 event in the GRIP ice core [GRIP Project Members, 1993] was a result of small-scale mixing by analyzing $\delta^{15}\text{N}$ of N_2 in the trapped gas, and interpreting the results in the context of a firm air model. Their conclusions are further supported by recent $\delta^{18}\text{O}_{\text{ice}}$ data of the NGRIP [North Greenland Ice Core Project Members, 2004] which shows that the temperature signals of the bottom part of the two previous Greenland Summit cores are clearly different from NGRIP prior to 101 ka on the GISP2 timescale (Figure 1).

[4] Chappellaz *et al.* [1997a] suggested that some samples from the GRIP and GISP2 cores have combined values of CH_4 concentration and $\delta^{18}\text{O}_{\text{atm}}$ that are consistent with an age assignment corresponding to the last interglacial (Marine Isotope Stage 5e). More recently, Landais *et al.* [2003] attempted to reconstruct the chronology of the disturbed section of the GRIP ice core and concluded that some ice samples are from the penultimate glacial maximum, between 190 ka and 130 ka. Their tentative climate reconstruction indicates that the glacial inception in Antarctica preceded that in Greenland.

[5] The goal of this study is to reconstruct a chronology for the bottom 10% of the Summit ice cores on the basis of CH_4 concentration and $\delta^{18}\text{O}_{\text{atm}}$ in the trapped gases, and partially validate this reconstruction with measurements of

triple isotope composition of O_2 . We are interested in using the results to reconstruct Greenland climate change prior to 101 ka, to the extent possible. We are also interested in characterizing the age distribution of the ice in the two cores as a contribution to glaciology. The chronology we create is based on a comparison of the combined records of CH_4 concentrations and $\delta^{18}\text{O}_{\text{atm}}$ in 77 samples [Chappellaz *et al.*, 1997a] from the disturbed section (2754 to 3038 m) of the GISP2 core, and includes 80 samples from the GRIP core [Landais *et al.*, 2003]. Samples from the Vostok ice core [Petit *et al.*, 1999] provide reference records of atmospheric composition versus time. We also use the NGRIP $\delta^{18}\text{O}_{\text{ice}}$ record to help constrain the chronology.

[6] In addition to CH_4 and $\delta^{18}\text{O}_{\text{atm}}$, other gas properties which change simultaneously in both hemispheres can serve as a tool for constructing a chronology of disturbed ice. $^{17}\Delta$ of O_2 is such a property. $^{17}\Delta$ of O_2 is defined as,

$$^{17}\Delta(\text{per meg}) = [\ln(\delta^{17}\text{O}_c/10^3 + 1) - 0.516 \cdot \ln(\delta^{18}\text{O}_c/10^3 + 1)] \cdot 10^3,$$

where δ_c indicates that the values have been corrected for gravitational fractionation. The atmospheric value of $^{17}\Delta$ has changed with time, primarily because of changes in the CO_2 concentration of air and the fertility of the planet [Luz *et al.*, 1999; Blunier *et al.*, 2002]. We report $^{17}\Delta$ for 25 samples of disturbed ice, and show that these values are consistent with our inferred ages.

2. CH_4 and $\delta^{18}\text{O}_{\text{atm}}$ Records and Methods for Determining $^{17}\Delta$ and Total Gas Content

[7] In this section, we derive virtual records of $\delta^{18}\text{O}_{\text{atm}}$ versus time and CH_4 versus time for Greenland ice cores prior to 101 ka. We do this derivation using data from the Vostok ice core, which extends back to about 420 ka [Petit *et al.*, 1999]. As described in the following section, we use the Vostok record to assign an age to each Greenland ice core sample on the basis of the CH_4 concentration and $\delta^{18}\text{O}_{\text{atm}}$ measured in that sample.

[8] Reconstruction of the $\delta^{18}\text{O}_{\text{atm}}$ record in Greenland is straightforward because O_2 in the atmosphere is well mixed. Its atmospheric residence time of ~ 1200 years [Bender *et al.*, 1994b] is far longer than the interhemispheric mixing time of 1 year. Thus $\delta^{18}\text{O}_{\text{atm}}$ over Antarctica is the same as $\delta^{18}\text{O}_{\text{atm}}$ over Greenland. Estimation of Greenland CH_4 from Vostok CH_4 is somewhat more complicated because most CH_4 sources, mainly wetlands, are concentrated in the tropics and the northern extratropics [Hein *et al.*, 1997]. As a result, the CH_4 concentration is higher in the Northern Hemisphere than in the Southern Hemisphere. Nevertheless, the temporal evolution of the methane concentrations is similar in both hemispheres [Blunier and Brook, 2001] because its lifetime (7 \sim 10 years [e.g., Khalil and Rasmussen, 1983; Prinn *et al.*, 1995; Lelieveld *et al.*, 1998]) is still longer than the interhemispheric mixing time (~ 1 year).

[9] To derive a correction for the gradient, we plot the concentration of methane in GISP2 with the concentration in synchronous gas samples from Vostok. The gas records of the two cores are aligned in the time interval 6.4–101 ka

by matching variations in $\delta^{18}\text{O}_{\text{atm}}$ [e.g., *Bender et al.*, 1994a], and by matching rapid changes in CH_4 [e.g., *Blunier and Brook*, 2001]. The plot is fit with the following equation:

$$\text{CH}_4^{\text{Greenland}}(t) = 0.99 \times \text{CH}_4^{\text{Vostok}}(t) + 49.36 \quad R^2 = 0.92 \quad (1)$$

where $\text{CH}_4^{\text{Vostok}}(t)$ is the methane concentration at time t in the Vostok ice core [*Petit et al.*, 1999] and $\text{CH}_4^{\text{Greenland}}(t)$ is the corresponding concentration in Greenland [*Blunier*

and *Brook*, 2001]. We then use this equation to calculate CH_4 in Greenland prior to 101 ka on the Vostok GT4 timescale [*Petit et al.*, 1999]. Note that *Landais et al.* [2003] used the equation; $\text{CH}_4^{\text{Greenland}}(t) = \text{CH}_4^{\text{Vostok}}(t)/0.93$ to account for the interhemispheric gradient. For comparison, equation (1) gives Greenland CH_4 concentrations of 445 and 643 ppbv for Vostok values of 400 and 600 ppbv, respectively. The corresponding values using the Landais equation are similar: 430 and 645 ppbv.

[10] The analytical technique for determining CH_4 and $\delta^{18}\text{O}_{\text{atm}}$ in the GISP2 ice core and the Vostok ice core was described by *Sowers et al.* [1997] and *Sowers et al.* [1989], respectively. The methodology for the GRIP ice core is given by *Landais et al.* [2003]. The CH_4 and $\delta^{18}\text{O}_{\text{atm}}$ data for the disturbed sections have been previously reported by *Bender et al.* [1994a], *Chappellaz et al.* [1997a], and *Landais et al.* [2003]. The pooled standard deviations for CH_4 and $\delta^{18}\text{O}_{\text{atm}}$ are reported to be ± 30 ppbv (2σ [*Sowers et al.*, 1997; E. Brook, unpublished results, 2004]) and $\pm 0.06\text{‰}$ (2σ [*Sowers et al.*, 1989, 1997]) respectively for both the GISP2 and Vostok ice core. They are estimated as ± 20 ppbv (2σ [*Landais et al.*, 2003]) and $\pm 0.08\text{‰}$ (2σ [*Landais et al.*, 2003]) respectively for the GRIP ice core. The uncertainty arising from calculating the interhemispheric gradient of methane is estimated as ± 38 ppbv (equivalent to a 96% prediction interval for the regression (1)). $^{17}\Delta$ measurements reported here were made using the method of *Blunier et al.* [2002]. The pooled standard deviation for $^{17}\Delta$ is ± 9.2 per meg (1σ). By adding errors quadratically, we estimate that the overall errors (2σ) associated with the CH_4 and $\delta^{18}\text{O}_{\text{atm}}$ for GISP2 ice core in this analysis are ± 57 ppbv and $\pm 0.08\text{‰}$ respectively, and errors (2σ) associated with the CH_4 and $\delta^{18}\text{O}_{\text{atm}}$ records for GRIP ice core are ± 52 ppbv and $\pm 0.1\text{‰}$ respectively. Total gas content was measured by isotope dilution mass spectrometry using an ^{38}Ar spike; $\text{O}_2/\text{N}_2/\text{Ar}$ ratios were taken as atmospheric for the purpose of this calculation. Precision is better than $\pm 1.5\%$ (1σ). We incorporate these errors into our age reconstruction calculations explained below.

3. Method for the Age Reconstruction

[11] The covariation of CH_4 concentration and $\delta^{18}\text{O}_{\text{atm}}$ is used to constrain ages of the GRIP and the GISP2 samples from the disturbed sections of these cores (Figure 2) [cf.

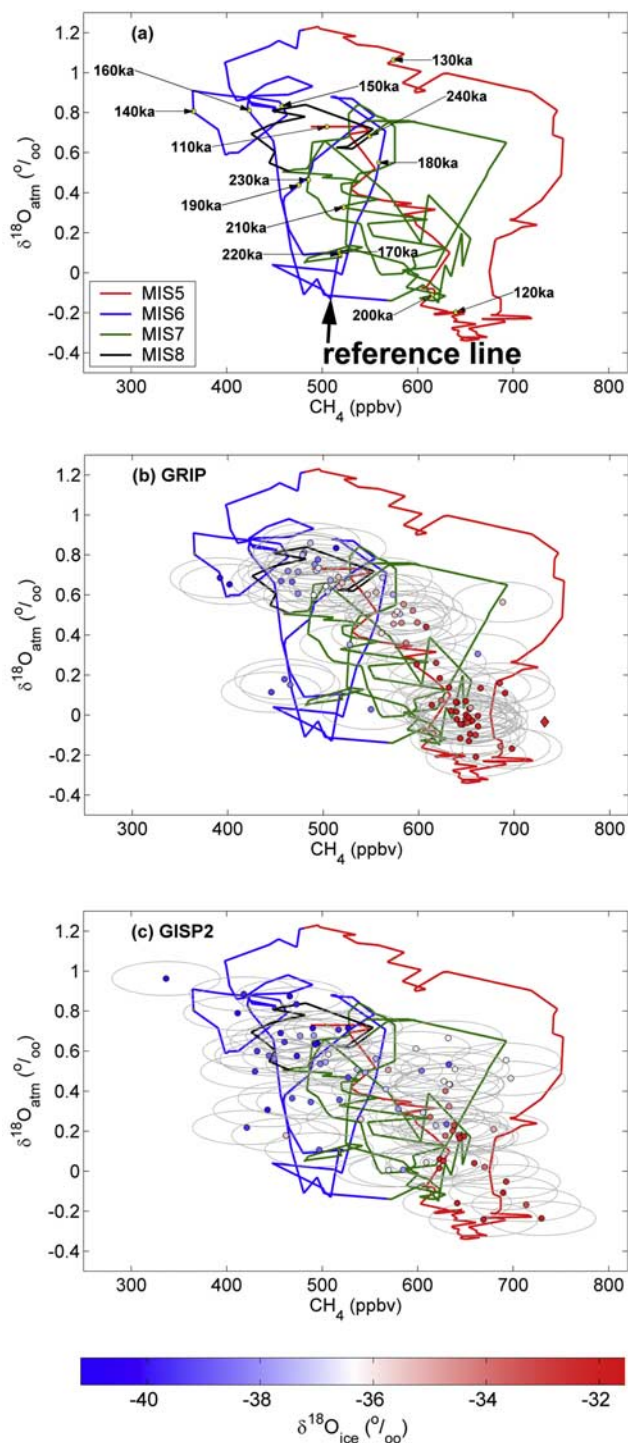


Figure 2. (a) Trajectory of CH_4 and $\delta^{18}\text{O}_{\text{atm}}$ records derived from the Vostok core between 110 ka and 250 ka on the GT4 timescale, when corrected for the interhemispheric gradient (called “reference line” in the text). Different line colors correspond to different marine isotope stages: red, MIS 5; blue, MIS 6; green, MIS 7; and black, MIS 8. (b) GRIP and (c) GISP2 data from the disturbed section of the core, shown as solid circles colored in shades of red and blue. Color represents $\delta^{18}\text{O}_{\text{ice}}$ at the same sample. Gray ellipses surrounding each data point are uncertainty ranges. A diamond shown in Figure 2b indicates that the sample is not compatible with any age between 250 ka and 101 ka, possibly because of its high methane concentration. Note that we define MIS 5 as starting at 133 ka, MIS 6 at 198 ka, and MIS 7 at 240 ka on the basis of a the Vostok plot of $\delta\text{D}_{\text{ice}}$ versus time (GT4 timescale).

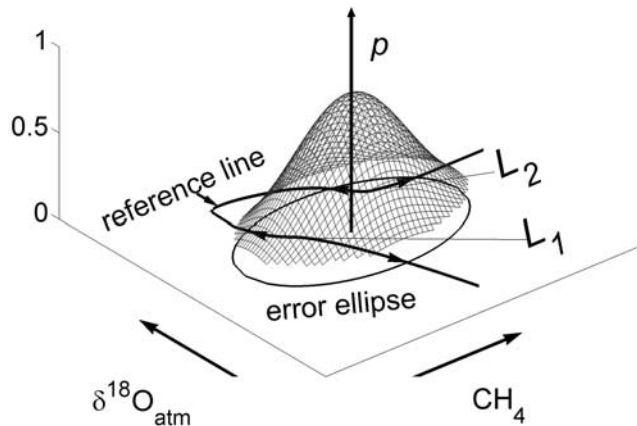


Figure 3. Schematic diagram illustrating a relationship between an error ellipse, L , and p in equation (4).

[Chappellaz *et al.*, 1997b; Landais *et al.*, 2003]. The “reference line” in Figure 2 refers to the curve of $\delta^{18}\text{O}_{\text{atm}}$ versus Greenland CH_4 concentration prior to 101 ka on the Vostok GT4 timescale [Petit *et al.*, 1999]. The basic idea is to identify the point on the “reference line” that best explains the CH_4 concentration and $\delta^{18}\text{O}_{\text{atm}}$ of each sample.

3.1. Identification of Compatible Ages for Each Sample

[12] Gas concentrations are often compatible with multiple age assignments, because the error envelopes of the data points frequently encompass more than one time period in $\text{CH}_4 - \delta^{18}\text{O}_{\text{atm}}$ space. Thus we first assign all compatible age ranges to each sample. This is done by seeking time t on the GT4 timescale which meets the following condition:

$$\frac{[\text{CH}_4^{\text{Greenland}}(t) - \text{CH}_4^{\text{disturbed}}(z)]^2}{[2\sigma(\text{CH}_4)]^2} + \frac{[\delta^{18}\text{O}_{\text{atm}}^{\text{Vostok}}(t) - \delta^{18}\text{O}_{\text{atm}}^{\text{disturbed}}(z)]^2}{[2\sigma(\delta^{18}\text{O}_{\text{atm}})]^2} \leq 1 \quad (2)$$

where $\text{CH}_4^{\text{Greenland}}(t)$ is the predicted methane concentration in the Northern Hemisphere defined in the equation (1) and $\delta^{18}\text{O}_{\text{atm}}^{\text{Vostok}}(t)$ is the Vostok $\delta^{18}\text{O}_{\text{atm}}$ value at time t . In this study, both $\text{CH}_4^{\text{Greenland}}$ and $\delta^{18}\text{O}_{\text{atm}}^{\text{Vostok}}$ are interpolated onto a time grid of 100 year interval. $\text{CH}_4^{\text{disturbed}}(z)$ and $\delta^{18}\text{O}_{\text{atm}}^{\text{disturbed}}(z)$ are methane concentration and $\delta^{18}\text{O}_{\text{atm}}$ value at depth z in a disturbed sample of either the GRIP or the GISP2 ice core, and $\sigma(\text{CH}_4)$ and $\sigma(\delta^{18}\text{O}_{\text{atm}})$ are one standard deviation for methane and $\delta^{18}\text{O}_{\text{atm}}$ described in the previous section, respectively. Applying 2σ error limits minimizes the likelihood that we erroneously exclude true age ranges. Once a gas age is assigned, we compute an ice age by adding an appropriate value for the gas age – ice age difference (Δ age). Δ age is calculated using the empirical model proposed by Herron and Langway [1980], which is reasonably well calibrated for the temperature and accumulation rate range of interest. Temperature and accumulation rate are two parameters necessary for this model. We estimate these parameters on the basis of $\delta^{18}\text{O}_{\text{ice}}$ values using equations shown by Johnsen *et al.* [1995] for temperature and by Dansgaard *et al.* [1993] for accumulation rate. Surface density is set to the modern observation. Estimated error

for Δ age is about 20%, between 40 years (interglacial maximum) and 200 years (glacial maximum) for Summit cores.

3.2. Rejection of Compatible Ages Inconsistent With the North GRIP Record

[13] If a disturbed sample has an ice age within the range of the NGRIP record (<123 ka), we examine whether the $\delta^{18}\text{O}_{\text{ice}}$ is compatible with this age assignment. We note that $\delta^{18}\text{O}_{\text{ice}}$ of GISP is related to that of NGRIP by the following regression:

$$\delta^{18}\text{O}_{\text{ice}}^{\text{Summit}}(t) = 0.73 \times \delta^{18}\text{O}_{\text{ice}}^{\text{NGRIP}}(t) - 9.37(\text{‰}) \quad R^2 = 0.81 \quad (3)$$

The points for this equation are derived by using visual wiggle matching to correlate the two cores, and projecting the GISP2 timescale [Meese *et al.*, 1994; Sowers *et al.*, 1993] onto the NGRIP record. A 96% prediction interval is $\pm 1.9\text{‰}$. If the $\delta^{18}\text{O}_{\text{ice}}$ of a GISP2/GRIP sample differs from the value of $\delta^{18}\text{O}_{\text{ice}}$ of Summit calculated from $\delta^{18}\text{O}_{\text{ice}}$ of the contemporaneous NGRIP sample and equation (3) by more than $\pm 1.9\text{‰}$, we reject this compatible ice and gas age assignment. 66 samples were affected by this criterion, all of which had at least one additional compatible age.

[14] In order to include NGRIP $\delta^{18}\text{O}_{\text{ice}}$ in our analysis, we need an NGRIP ice chronology that is consistent with the Vostok chronology for the interval predating the oldest undisturbed Summit ice. We employ a chronology recently proposed by Landais *et al.* [2006] in which they used $\delta^{18}\text{O}_{\text{atm}}$ record of NGRIP to compare with Vostok $\delta^{18}\text{O}_{\text{atm}}$. Their chronology is further supported by methane record of Vostok and NGRIP around Interstadial Event 24, when atmospheric methane increased rapidly at 105.3 ka.

3.3. Determination of Most Likely Age Range

[15] If a sample has multiple age ranges which satisfy equation (2) and a $\delta^{18}\text{O}_{\text{ice}}$ value that is compatible with NGRIP data, we then search a “most likely” age range, which maximizes the following term:

$$P_{\text{ice}} \times \int p \frac{dL}{dL/dt} \quad (4)$$

[16] L is the geometrical length of a segment of the reference line intersecting an error ellipse. Figure 3 illustrates the case where the locus of $\delta^{18}\text{O}_{\text{atm}}$ versus CH_4 points passes through the sample’s error ellipse at 2 times, corresponding to line segments L_1 and L_2 . dL is divided by the rate of change thereby favoring line segments falling within the error ellipse for longer times. p is a probability that values within the error ellipse fall along the intersecting segment of the reference line, and is estimated by assuming the Gaussian distribution. In Figure 3, it is represented by the height (p) of the probability surface. Thus the integral term favors (1) candidate ages corresponding to longer times within the error ellipse and (2) candidate ages falling near the center of an ellipse as opposed to the edges. The calculation is made after rescaling both $\text{CH}_4^{\text{Greenland}}(t)$ and $\delta^{18}\text{O}_{\text{atm}}^{\text{Vostok}}(t)$ to a mean of zero and a standard deviation of one. P_{ice} is probability of finding ice of a given age, and

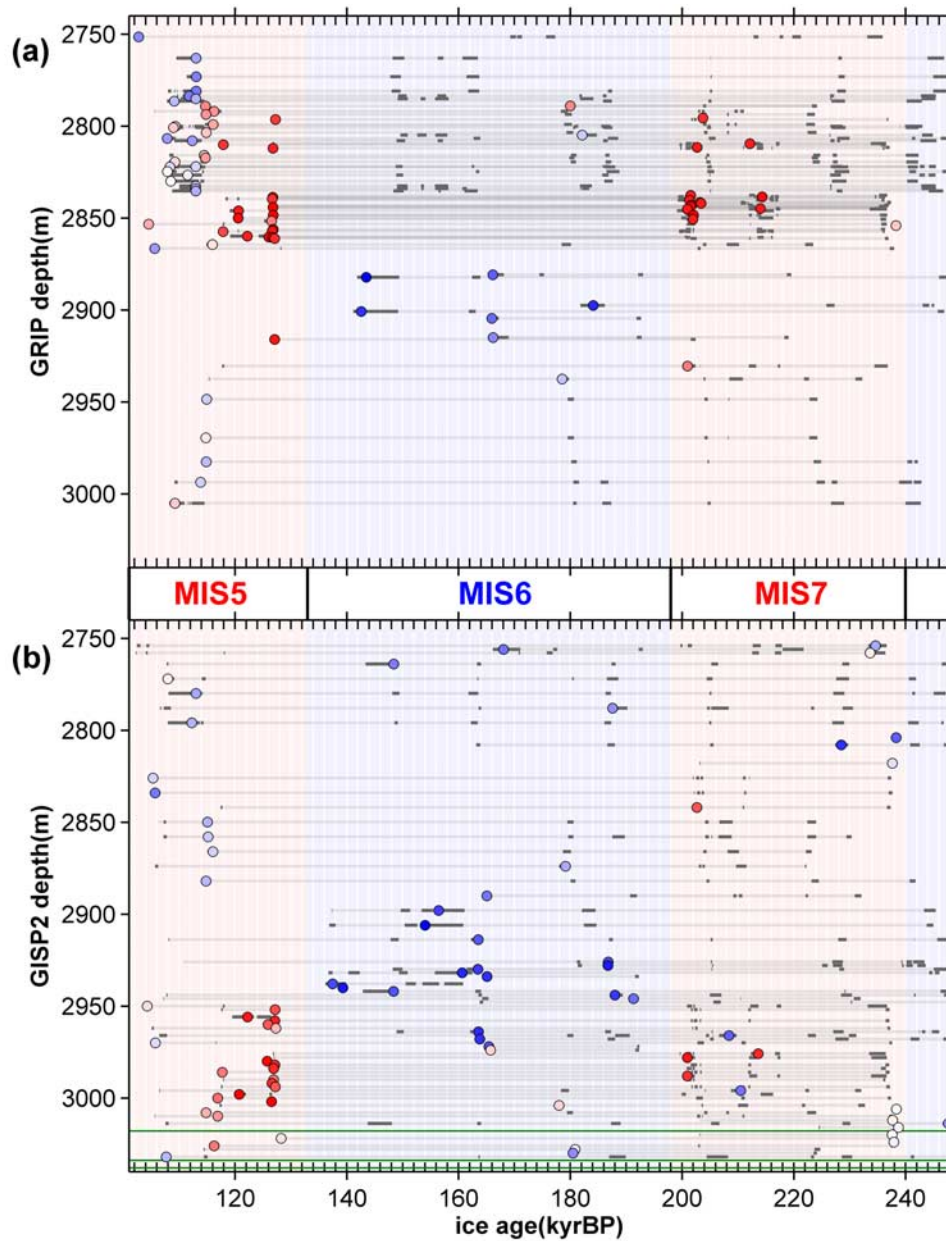


Figure 4. Reconstructed age-depth relationship for (a) the GRIP ice core and (b) the GISP2 ice core. Ages plotted are the “best estimate ages” with their face colors indicating $\delta^{18}\text{O}_{\text{ice}}$ (scale is the same as Figure 2). Gray bars indicate all possible age ranges. Three green lines in Figure 4b correspond to samples having methane concentration higher than 800 ppbv.

is defined as the fraction of ice of a given age in the basal section of a hypothetical, undisturbed, Summit ice core. P_{ice} depends on accumulation rate and thinning. To calculate P_{ices} , we utilize the thinning function and the equation given by Dansgaard *et al.* [1993], which computes past accumulation rate of Greenland from temperature. This temperature curve is estimated by invoking the empirical relationship between atmospheric CH_4 and Summit temperature. We estimate the virtual Summit temperature curve from the Vostok CH_4 curve by rescaling it linearly so that $\delta^{18}\text{O}_{\text{ice}} = -32\text{‰}$ at the last interglacial CH_4 maximum and $\delta^{18}\text{O}_{\text{ice}} = -44\text{‰}$ at the penultimate glacial CH_4 minimum (corresponding to Marine Isotope Stage 6). Note that P_{ice} is strongly influenced by thinning. How-

ever, small changes in estimated temperature would not cause any significant change in our results.

3.4. Determining the “Best Estimate” Age

[17] The “best estimate age” is found within a “most likely” age range. The best estimate age is defined as t_{best} which minimizes d , a distance between a sample and the reference line, represented as;

$$d = \sqrt{[{}_n\text{CH}_4^{\text{Greenland}}(t_{\text{best}}) - {}_n\text{CH}_4^{\text{disturbed}}(z)]^2 + [{}_n\delta^{18}\text{O}_{\text{atm}}^{\text{Vostok}}(t_{\text{best}}) - {}_n\delta^{18}\text{O}_{\text{atm}}^{\text{disturbed}}(z)]^2} \quad (5)$$

The subscript n indicates that the term is normalized as described above (mean = 0, standard deviation = 1). In this

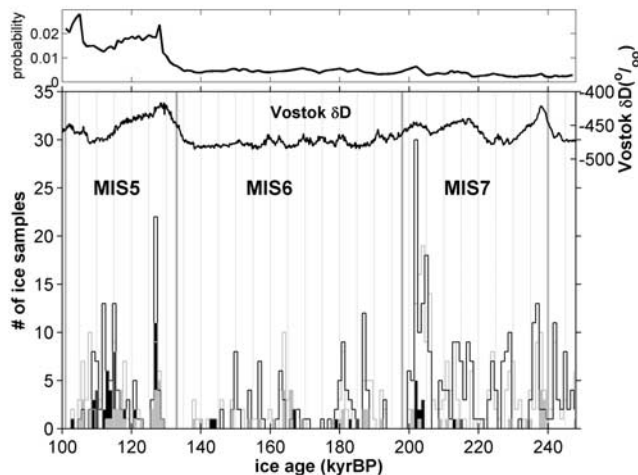


Figure 5. Number of ice samples found in each of 1000 year interval starting from 110 ka backward. Black indicates GRIP samples, and gray indicates GISP2 samples. The “best estimate” ages are plotted as solid bars, and “all possible” age ranges are plotted as open bars. Also shown is Vostok δD_{ice} . Top plot shows P_{ice} versus age.

approach, the “best estimate age” is the age of the point on the $\delta^{18}O_{atm} - CH_4$ curve lying closest to the observations.

[18] We searched for the best estimate age using equations (2)–(5), examining fits in increment of 100 years moving from 101 ka backward.

[19] We repeated this exercise eliminating the dL/dt term from equation (4) (results not shown). In this case, the probability of an age is weighted by the length of the $\delta^{18}O_{atm} - CH_4$ line within the error ellipse, rather than the length of time. 103 out of 153 samples had the same “best estimate” ages with the two approaches.

4. Results and Discussion

4.1. Caveats

[20] We restricted our age search to a period younger than 250 ka because, if there were no basal mixing, almost all ice would be younger than this age [Dansgaard *et al.*, 1993]. We cannot exclude the possibility that much older ice is present, but consider it unlikely. Our analysis excludes three GISP2 samples with methane concentrations higher than 800 ppbv. Two of these samples are from the deepest part of the GISP2 core and the third is also deeper than 3000 m. 800 ppbv exceeds the atmospheric CH_4 concentration of the past 400 ka prior to the period of industrialization [Petit *et al.*, 1999]. We concluded that the methane concentrations in these samples might have been altered by methane from fermentation of organic matter below the ice [Souchez *et al.*, 1995]. There is one GRIP sample shown as a diamond in Figure 2 that is not consistent with any age between 101 ka and 250 ka; its 2σ error envelope lies just outside the CH_4 and $\delta^{18}O_{atm}$ curve at 125.5 ka.

4.2. Age Distribution of Disturbed Ice

[21] Figure 2 shows the covariation of CH_4 and $\delta^{18}O_{atm}$ in Greenland as inferred from Vostok ice core data. Superimposed on this reference line are data for samples from the

disturbed section of the GISP2 and GRIP cores. Fill color reflects $\delta^{18}O_{ice}$, a qualitative proxy for temperature in Greenland. On the basis of the data set shown in Figure 2 and the age reconstruction method described in the previous section, we derived the age – depth relationship shown in Figure 4. In this plot, colored points are “best estimate ages,” and colors reflect $\delta^{18}O_{ice}$ (warmer colors indicate heavier values). Solid gray lines give other compatible ages. Most samples have $\delta^{18}O_{atm}$ and CH_4 concentrations compatible with several discrete age ranges. We find that there are eight GISP2 samples and two GRIP samples assigned unique ages between 101 ka and 250 ka. Among those ten, three GISP2 samples and one GRIP sample are dated between 239 ka and 237 ka. Thus we conclude that the oldest ice in the bottom sections is at least 237 ka, which corresponds to Marine Isotope Stage (MIS) 7. Of samples with multiple compatible ages, one GRIP and four more GISP2 samples are dated to MIS 7 or older. Four uniquely dated GISP2 samples and one uniquely dated GRIP sample lie at the end of the penultimate glacial and at the beginning of the last interglacial.

4.3. Underrepresented Intervals of Time

[22] Figure 5 shows the number of samples consistent with each 1 kyr interval working back from 100 ka. Both “best estimate” ages and “all compatible” age ranges are plotted. We found that best estimate ages of 68% of GRIP samples and 42% of GISP2 samples correspond to MIS 5, 11% of GRIP samples and 34% of GISP2 samples correspond to MIS 6, 20% of GRIP samples and 22% of GISP2 samples correspond to MIS 7, and 0% of GRIP samples and 3% of GISP2 sample correspond to MIS 8 (Table 1). Some age intervals are underrepresented. For example, there are at most four samples (2%) with compatible ages between 125 ka and 121 ka, a period presumably corresponding to the warmest period during the last interglacial in Greenland. Further no ice sample has compatible ages between 137 ka and 130 ka, which probably corresponds to the early stage of Termination II in Greenland.

[23] In order to examine if underrepresentation for these two intervals is statistically significant, we conducted the following experiment. First we divide the whole age range into multiple age intervals of equal sampling probability, given our assumed curves of accumulation rate and thinning versus age (P_{ice}). Intervals are thus longer when accumulation is slow and thinning is extensive. We then randomly distribute 154 samples among these intervals. When assuming no basal mixing, the probability that a single sample of ice comes from intervals corresponding to 125–121 ka and 137 ka–130 ka are 0.13 and 0.048 respectively. Then we calculate probabilities of finding less than three samples out of 154 samples for an interval corresponding to $\int P_{ice} = 0.127$ (125 ka–121 ka) and (2) no sample for an interval corresponding to $\int P_{ice} = 0.048$ (137 ka–130 ka) along a whole age range. We found that $p < 0.05$ for 125 ka–121 ka and $p < 0.1$ for 137 ka–130 ka. Therefore we conclude that those intervals are significantly underrepresented at a (1) 5% and (2) 10% significance level. A smaller Greenland ice sheet during the Eemian [Cuffey and Marshall, 2000] may have contributed to 121–125 ka. Although we do not understand the cause of underrepresentation, the observation would seem to reflect

Table 1. Summary of Age Distribution for the Samples From the Disturbed Sections (in the “Standard” Column)^a

	Standard	No Thinning	No NGRIP Test	P_{ice}
	<i>GRIP</i>			
MIS-5	54 (0.68)	20 (0.25)	71 (0.90)	(0.55)
MIS-6	9 (0.11)	8 (0.10)	7 (0.09)	(0.29)
MIS-7	16 (0.20)	46 (0.58)	1 (0.01)	(0.14)
MIS-8	0 (0.00)	5 (0.06)	0 (0.00)	(0.02)
Total	79 (1.00)	79 (1.00)	79 (1.00)	(1.00)
	<i>GISP2</i>			
MIS-5	31 (0.42)	12 (0.16)	53 (0.72)	(0.55)
MIS-6	25 (0.34)	20 (0.27)	15 (0.20)	(0.29)
MIS-7	16 (0.22)	39 (0.53)	4 (0.05)	(0.14)
MIS-8	2 (0.03)	3 (0.04)	2 (0.03)	(0.02)
Total	74 (1.00)	74 (1.00)	74 (1.00)	(1.00)

^aAlso shown are sensitivity of age distribution to P_{ice} in equation (3) (in the “no thinning” column) and to NGRIP chronology (in the “no NGRIP test” column). Numbers indicated in parentheses are fractions. The “ P_{ice} ” column shows fractions of ice expected if there is no basal mixing.

important information about the accumulation or disturbance history of Summit ice, and merits further attention.

4.4. Sensitivity of the Calculations to Assumptions

[24] In order to examine the sensitivity of our results to various assumptions, we conducted and report the following two analyses.

[25] First, we conducted a sensitivity experiment to see how the term P_{ice} in equation (4) affects the reconstructed

chronology. In this test, we calculated best ages for all samples without reference to thinning and accumulation rate (i.e., setting $P_{ice} = 1$). Not surprisingly, the best ages for many samples become older. In fact, more than 50% of GISP and GRIP samples are dated in MIS 7 and MIS 8 (Table 1) although we think that thinning makes the presence of many MIS 7/MIS 8 samples unlikely.

[26] Second, we tested the sensitivity of our dates to the “NGRIP test.” The NGRIP $\delta^{18}O_{ice}$ versus time curve is important because it determines which disturbed samples we exclude from dates corresponding to the glacial inception (101–123 ka), because their $\delta^{18}O_{ice}$ values are incompatible with NGRIP values. When omitting the NGRIP test, we found that 90% of GRIP samples and 72% of GISP2 samples are compatible with MIS 5. Figure 6a shows reconstructed $\delta^{18}O_{ice}$ when omitting the NGRIP test. Very high $\delta^{18}O_{ice}$ values are found around 105 ka in this reconstruction. Such values are improbable at this time. For example, there is no North Atlantic record showing interglacial equivalent warmth right after the last glacial inception [e.g., Sanchez Goni et al., 1999; Gouzy et al., 2004].

4.5. The $^{17}\Delta$ of O_2 Test for the Reconstructed Chronology

[27] Twenty five new measurements of $^{17}\Delta$ of O_2 from the bottom section of the GISP2 core were made to test the reconstructed chronology (Table 2). Most GISP2 $^{17}\Delta$ values

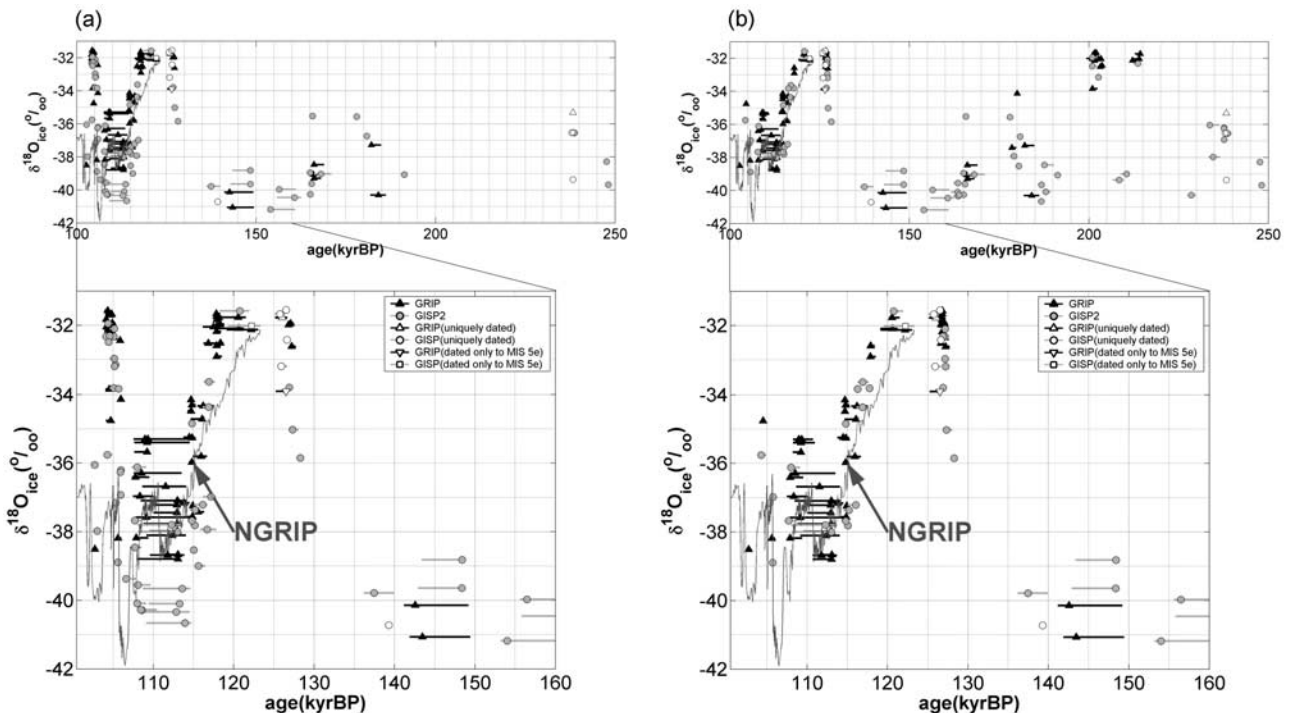


Figure 6. The $\delta^{18}O_{ice}$ of the GRIP and the GISP2 ice cores versus age. Solid triangles (GRIP) and shaded circles (GISP2) are plotted against the best estimate ages. Open triangles (up) (GRIP) and open circles (GISP2) are the ten samples with unique ages between 101 ka and 250 ka. An open triangle (down) (GRIP) and an open square (GISP2) have multiple age ranges, but all fall within isotope substage 5e. Solid and shaded bars indicate “most likely” age ranges for GRIP samples and GISP2 samples, respectively. NGRIP $\delta^{18}O_{ice}$ is also shown as a shaded curve. (a) Without using the NGRIP test and (b) with the NGRIP test.

Table 2. New Measurements of $^{17}\Delta$ of O_2 of Twenty Five Samples From the Disturbed Bottom Section of the GISP 2 Core

Depth, m	$^{17}\Delta$, per meg
2906	28
2926	29
2946	11
2960	6
2962	7
2964	51
2966	15
2972	4
2974	69
2978	1
2982	8
2986	11
2988	0
2990	7
2992	17
2993.9	41
2996	7
3000	21
3002	2
3004	1
3006	4
3008	10
3020	15
3030	15
3032	32

plotted versus the best estimate ages are within $\pm 1\sigma$ of the Vostok $^{17}\Delta$ record [Blunier *et al.*, 2002; M. Bender *et al.*, unpublished data, 2005], although we did not use $^{17}\Delta$ of O_2 to constrain our chronology. This general agreement between the Vostok $^{17}\Delta$ of O_2 and GISP2 $^{17}\Delta$ of O_2 adds some confidence in the reconstructed age scale (Figure 7). However, we note that $^{17}\Delta$ of O_2 cannot be a strong third independent parameter to constrain ages because it correlates with CH_4 and uncertainty is relatively large with respect to variations.

[28] In the following sections, we discuss reconstructions of the climate proxy records: $\delta^{18}O_{ice}$, total gas content, and glaciochemistry. We limit our interpretation to apparently robust features. However, there is the caveat that most of our ages are probabilistic rather than unique. Therefore some samples are almost certainly not correctly dated. Events are robust only when they are defined by multiple samples and/or by some of the 10 samples that are uniquely dated.

4.5.1. The $\delta^{18}O$ of Ice

[29] Figure 6b shows the reconstruction of $\delta^{18}O_{ice}$, or proxy temperature. Eight open circles (GISP2) and two open triangles (up) (GRIP) show the samples assigned unique ages. Four open circles and one open triangle (up) found between 127 ka and 125 ka in the bottom panel of Figure 6b indicate that last interglacial (MIS 5e) ice exists in the Greenland Ice cores, and the open circle found at 139 ka indicates that penultimate glacial (MIS 6) ice exists in the GISP ice core, which supports the conclusions by Landais *et al.* [2003]. Of samples with multiple compatible ages, one GRIP sample and one GISP2 sample can be dated only to ages between 118 and 127 ka, during MIS 5e (an open square and an open triangle (down) in Figure 6b). Thus there are at least seven GISP2 and GRIP samples that are uniquely dated to the interval between 118 ka and 127 ka. The average $\delta^{18}O_{ice}$ value for these seven samples is $-32.4 \pm$

0.9‰, and the average value for five samples uniquely dated between 127 ka and 124 ka (the earlier part of last interglacial in central Greenland on our timescale) is $-32.1 \pm 0.7\%$. In comparison, the average $\delta^{18}O_{ice}$ value for Holocene GISP2/GRIP ice is $-34.9 \pm 0.7\%$. No samples out of 2754 Holocene GRIP samples, and only 1.8% out of 14307 Holocene GISP2 samples, have $\delta^{18}O_{ice} \geq -32.1\%$. Further, the null hypothesis, $H_0: \mu(\text{Holocene } \delta^{18}O_{ice}) = \mu(\text{MIS 5e } \delta^{18}O_{ice})$ is rejected at $\alpha = 0.01$ in favor of an alternative hypothesis, $H_a: \mu(\text{Holocene } \delta^{18}O_{ice}) < \mu(\text{MIS 5e } \delta^{18}O_{ice})$ in the t-test. Assuming that $\delta^{18}O_{ice}$ mainly reflects local temperature, these results indicate that central Greenland was warmer than Holocene at the early stage of the last interglacial. A similar high $\delta^{18}O_{ice}$ value is also found at the very bottom of NGRIP. This ice presumably records warm temperatures just preceding the glacial cooling at the end of MIS 5e [North Greenland Ice Core Project Members, 2004; Landais *et al.*, 2006].

[30] In four samples from the GISP2 core and one sample from the GRIP core between 126 ka and 127 ka (open circles and an open triangle (up) plotted in Figure 6b), $\delta^{18}O_{ice}$ varies by about 1.6‰, within the range of Holocene variability.

4.5.2. Total Gas Content

[31] Total gas content in ice cores mainly relates to elevation at which air was occluded. Climatic conditions could also affect total gas content, but its impact would be smaller. For example, Raynaud *et al.* [1997] showed that the total gas content of the GRIP core fell during the last termination. They interpreted lower values of total gas content as higher elevation, due to the decrease in air density with altitude. They concluded that the change indicated a deglacial increase in ice sheet thickness, which was attributed to warmer temperatures and increased precipitation. Using GCMs, Krinner *et al.* [2000] reached the conclusion that Raynaud *et al.* [1997] underestimated the

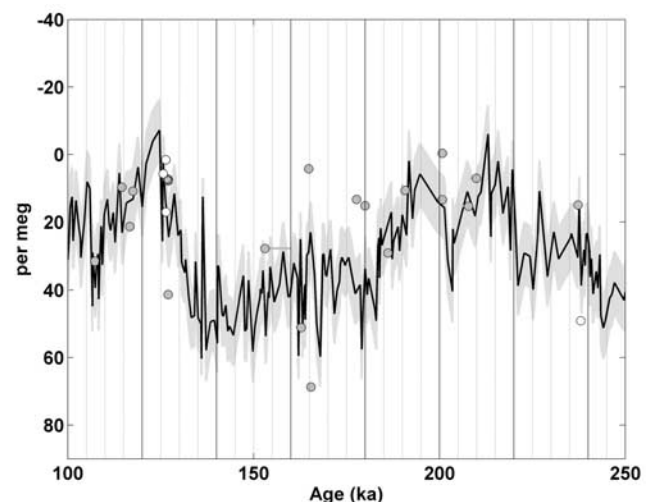


Figure 7. The $^{17}\Delta$ of O_2 [Blunier *et al.*, 2002; M. Bender *et al.*, unpublished data, 2005] versus time plotted (solid line) with $\pm 1\sigma$ (shaded area). Shaded circles are $^{17}\Delta$ of O_2 of the disturbed section of the GISP2 core plotted versus best estimate ages. Four open circles are uniquely dated samples.

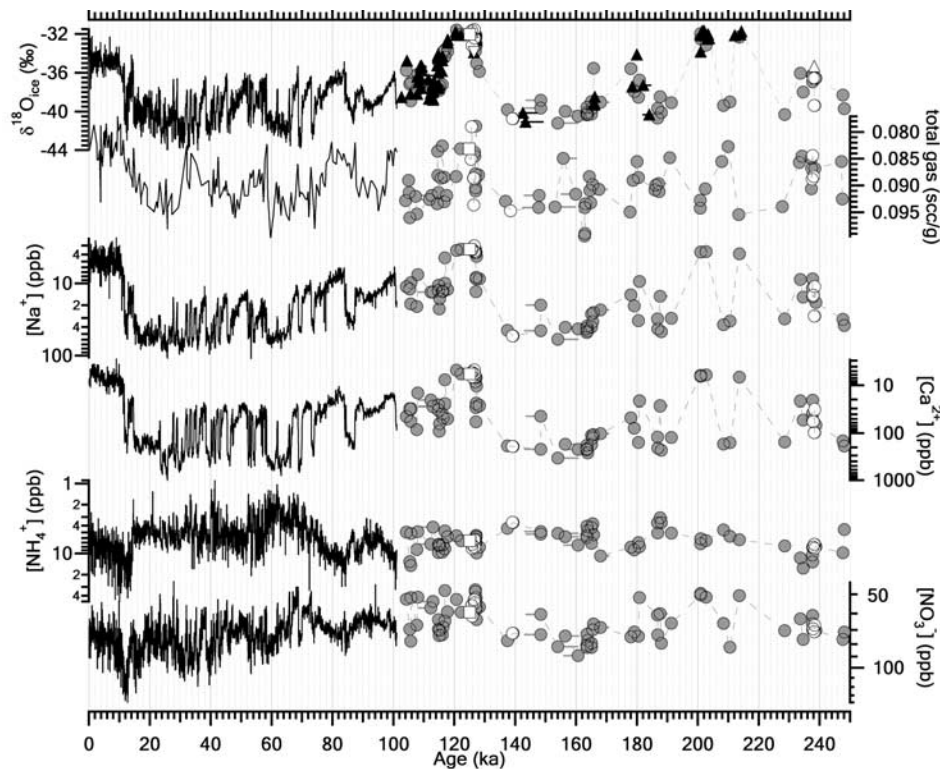


Figure 8. Records of $\delta^{18}\text{O}_{\text{ice}}$ (GRIP and GISP2), total gas content (GISP2), and glaciochemical species (GISP2). Na^+ , Ca^{2+} , NH_4^+ , and NO_3^- are plotted here on a log scale [Mayewski *et al.*, 1997]. The scale is reversed for total gas content, Na^+ , Ca^{2+} , NH_4^+ , and NO_3^- . Symbols for the reconstructed part of the records are the same as in Figure 6. Records between 0 and 110 ka are plotted on the timescales of Meese *et al.* [1994] and Sowers *et al.* [1993].

elevation change of Summit from LGM to Holocene because they did not consider other climate factors such as the surface pressure and the mean surface temperature. We assume that total gas content mainly reflects changes in elevation, but do not quantitatively interpret this property as we do not know how it is affected by climatic factors between 101 ka and 250 ka. Figure 8 shows that four samples uniquely dated at the beginning of the last interglacial period have a wide range of total gas content. Yet, each of these four samples has a lower total gas content than the sample uniquely dated at the beginning of Termination II. Total gas content of the penultimate glacial maximum is similar to that of the last glacial maximum, but total gas content of the last interglacial and the penultimate interglacial seems slightly higher than that of the current interglacial. Then as Greenland cools between 119 and 112 ka, total gas content quickly returns to glacial values. Finally, total gas content appears to decrease slightly at the time of the NGRIP warming at 102 ka. The main implication of these results is that, during the last interglacial period, total gas content was less than during the preceding glacial, implying a rise in elevation of Summit, Greenland, during Termination II.

4.5.3. Glaciochemical Species

[32] The time courses of eight glaciochemical species (Cl^- , NO_3^- , SO_4^{2-} , Na^+ , K^+ , NH_4^+ , Mg^{2+} , Ca^{2+}) and dust of the GISP2 core are considered in this study as well. Na^+ is mostly derived from sea salt and Ca^{2+} is considered to be

of continental origin [Mayewski *et al.*, 1997]. Four glaciochemical species (Cl^- , SO_4^{2-} , K^+ , Mg^{2+}) which are not shown in Figure 8 have profiles similar to $[\text{Na}^+]$. Five GISP2 samples (open circles) between 125 ka and 140 ka indicate a decrease in anion and cation concentrations, except for $[\text{NH}_4^+]$, across Termination II. Ammonium, on the other hand, shows a slight increase across Termination II. This sense and magnitude of the relationship between temperature and glaciochemical species is essentially the same as in records younger than 101 ka [Mayewski *et al.*, 1997].

[33] Variations of Cl^- , SO_4^{2-} , Na^+ , K^+ , Mg^{2+} , Ca^{2+} and probably NO_3^- concentrations reflect in part the strength of atmospheric circulation in the polar region of the Northern Hemisphere [Mayewski *et al.*, 1997]. Thus the atmospheric circulation was stronger at 139 ka, before the beginning of Termination II, and weaker during the warm last interglacial period. Interpretation of ammonium data is more complicated. Ammonium mostly comes from continental biogenic sources [Mayewski *et al.*, 1997]. Therefore ammonium variations reflect the extent of biogenic activity as well as the intensity of atmospheric circulation which transports it to the higher latitudes. Increased ammonium toward the end of Termination II was presumably due to increased biogenic activity during the warm period.

4.5.4. The $\delta^{15}\text{N}$ of N_2

[34] If temperature change at the surface is gradual, $\delta^{15}\text{N}$ of N_2 can be considered as a good indicator of

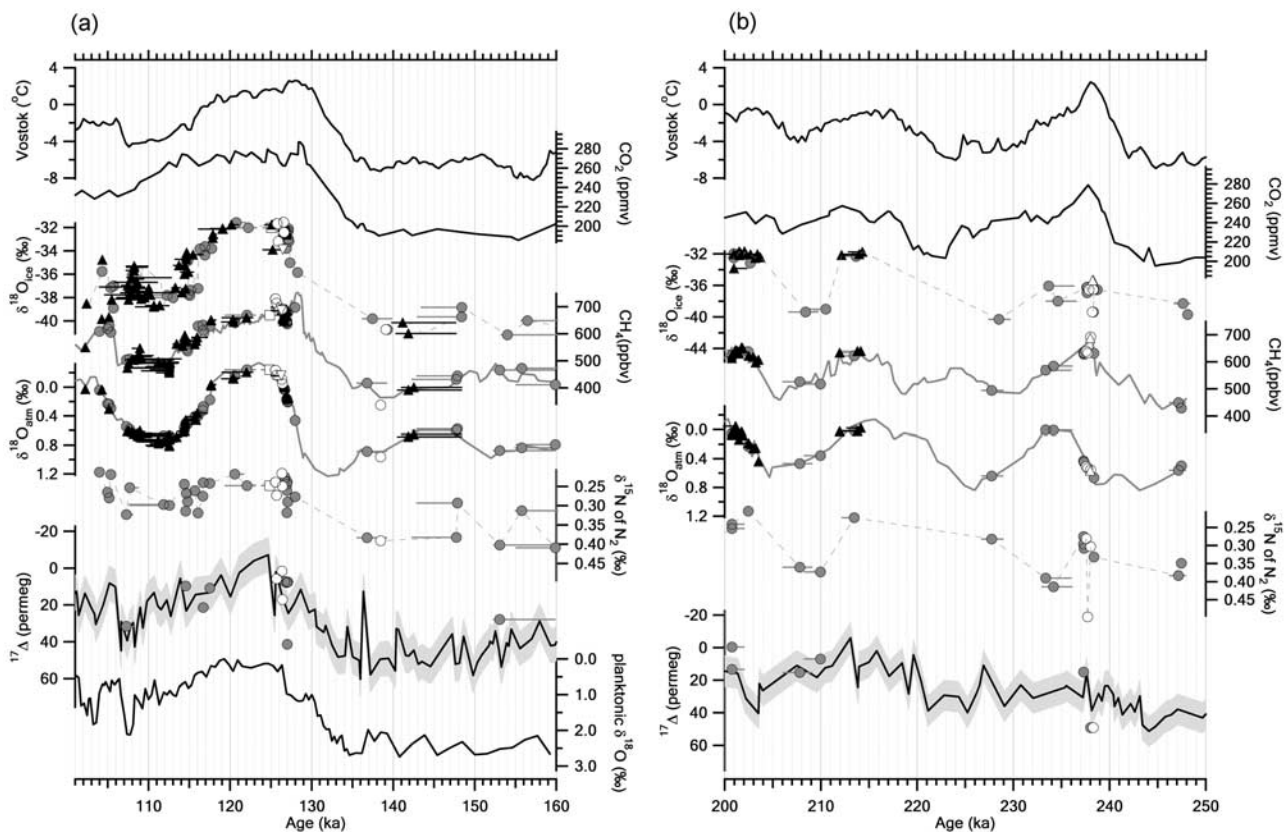


Figure 9. Greenland $\delta^{18}\text{O}_{\text{ice}}$ (temperature proxy) compared to Vostok temperature [Petit *et al.*, 1999]. Also shown are CO_2 [Petit *et al.*, 1999], the reconstructed Greenland methane record, the reconstructed $\delta^{18}\text{O}_{\text{atm}}$ record, $\delta^{15}\text{N}$ of N_2 , and $^{17}\Delta$ of O_2 [Blunier *et al.*, 2002; M. Bender *et al.*, unpublished data, 2005]. Shaded circles and solid triangles are the measurements of the disturbed section of the GISP2 core and the GRIP core, respectively, plotted versus best estimate ages. Open triangles (up) (GRIP) and open circles (GISP2) are uniquely dated samples. An open triangle (down) (GRIP) and an open square (GISP2) have multiple age ranges, but all fall within isotope substage 5e. Shaded area plotted with $^{17}\Delta$ of O_2 record shows $\pm 1\sigma$. Note that scale is reversed for $\delta^{18}\text{O}_{\text{atm}}$, $^{17}\Delta$ of O_2 , and planktonic $\delta^{18}\text{O}$. (a) Between 160 ka and 100 ka and (b) between 250 ka and 200 ka. The $\delta^{18}\text{O}$ of planktonic foraminifera from the Iberian margin (MD952042) is also plotted for Figure 9a [Sanchez Goni *et al.*, 1999].

close-off depth (more precisely, “lock-in” depth) at a high accumulation site such as Summit, since the convective zone in such a site is found to be minimal [Schwander *et al.*, 1993; Battle *et al.*, 1996; Severinghaus *et al.*, 2001]. Smaller enrichments in ^{15}N are observed at sites with shallower close-off depths [Sowers *et al.*, 1989], which result from warmer temperature. For example, reduction of $\delta^{15}\text{N}$ of N_2 between 139 ka and 127 ka is associated with warming in Greenland during this period (Figure 9a).

[35] When surface temperature changes abruptly, this is not exactly the case. Severinghaus *et al.* [1998] and Severinghaus and Brook [1999] showed that $\delta^{15}\text{N}$ of N_2 was enriched by thermal fractionation when surface temperature rose abruptly. For example, we observe a sample with heavy $\delta^{15}\text{N}$ of N_2 ($\sim 0.49\%$) between 238 ka and 237 ka, and this sample might have been fractionated by thermal in addition to gravitational fractionation. At this time (Termination III), we also find a relatively sharp increase of methane, consis-

tent with the observation for the past 110,000 years that methane concentrations rise abruptly at times of rapid Greenland warming.

4.5.5. Termination II

[36] Our reconstruction suggests that the last part of deglacial warming of Summit continued between 128 ka and 126 ka, while CH_4 rose to the interglacial maximum by 128 ka (Figure 9a). In fact, methane concentrations were decreasing slightly when Greenland was still warming according to the reconstruction in this study. This temperature- CH_4 relationship is similar to that observed in Termination I, where CH_4 increased abruptly at the same time as the temperature rise at the end of Younger Dryas period, but temperature continued to rise for the next few thousand years after CH_4 reached its interglacial maximum. The last part of Terminations I and II in Greenland probably corresponds to the additional warming in Greenland caused by melting of boreal ice sheets, which caused albedo to decrease.

[37] We also note that a “climatic pause” has been identified which divides Termination II into two steps observed at the Iberian margin [Sanchez Goni et al., 1999; Gouzy et al., 2004] (Figure 9a) and at the California margin [Cannariato and Kennett, 2005]. A warming trend between 128 ka and 126 ka in our reconstruction might correspond to the latter step of Termination II in the North Atlantic. In other words, the first step of Termination II might involve a CH₄ rise to the interglacial maximum, and the second step is warming associated with ice sheet melting.

5. Conclusions

[38] A chronology for the bottom section of the GRIP and GISP2 cores was reconstructed on the basis of the concentration of CH₄ in trapped air and the δ¹⁸O of O₂ assuming that no samples were older than 250 ka. The oldest ice in the Summit cores is at least 237 ka, which corresponds to the penultimate interglacial period. With this assumption, we have uniquely dated seven samples to MIS 5e, the last interglacial period, one sample to MIS 6, the penultimate glacial period, and nine samples to MIS 7. Ages have been partly validated with data on the ¹⁷Δ of O₂. The age reconstruction in this study supports previous suggestions that Summit ice from the last interglacial had a higher δ¹⁸O than Holocene samples indicating warmer temperatures. Changes of the total gas content, as well as in glaciochemical species across Terminations II and III in central Greenland, were similar to Termination I. According to our reconstruction, the pattern of deglacial temperature rise at Termination II is similar to that observed at Termination I: postglacial temperatures continue to rise for several thousand years after the abrupt increase in CH₄, indicating additional warming associated with melting of boreal ice sheets and the decrease in albedo linked to warming of the deglaciaded continents.

[39] **Acknowledgments.** The authors would like to thank Jim White for GISP2 δ¹⁸O_{ice} data, Bruce Barnett for technical assistance, and Thomas Blunier for helpful discussion. This work was supported by a gift from the Gary Comer Foundation and the Office of Polar Programs, NSF.

References

- Battle, M., et al. (1996), Atmospheric gas concentrations over the past century measured in air from firn at the South Pole, *Nature*, **383**, 231–235.
- Bender, M., T. Sowers, M.-L. Dickson, J. Orchardo, P. Grootes, P. Mayewski, and D. Meese (1994a), Climate connections between Greenland and Antarctica during the last 100,000 years, *Nature*, **372**, 663–666.
- Bender, M., T. Sowers, and L. Labeyrie (1994b), The Dole effect and its variations during the last 130,000 years as measured in the Vostok ice core, *Global Biogeochem. Cycles*, **8**, 363–376.
- Blunier, T., and E. J. Brook (2001), Timing of millennial-scale climate change in Antarctica and Greenland during the Last Glacial Period, *Science*, **291**, 109–112.
- Blunier, T., B. Barnett, M. L. Bender, and M. B. Hendricks (2002), Biological oxygen productivity during the last 60,000 years from triple oxygen isotope measurements, *Global Biogeochem. Cycles*, **16**(3), 1029, doi:10.1029/2001GB001460.
- Brook, E. J., T. Sowers, and J. Orchardo (1996), Rapid variations in atmospheric methane concentration during the past 110,000 years, *Science*, **273**, 1087–1091.
- Cannariato, K. G., and J. P. Kennett (2005), Structure of the penultimate deglaciation along the California margin and implications for Milankovitch theory, *Geology*, **33**, 157–160.
- Chappellaz, J., T. Blunier, D. Raynaud, J. M. Barnola, J. Schwander, and B. Stauffer (1993), Synchronous changes in atmospheric CH₄ and Greenland climate between 40 and 8 ky BP, *Nature*, **366**, 443–445.
- Chappellaz, J., E. Brook, T. Blunier, and B. Malaize (1997a), CH₄ and δ¹⁸O of O₂ records from Antarctic and Greenland ice: A clue for stratigraphic disturbance in the bottom part of the Greenland Ice Core Project and the Greenland Ice Sheet Project 2 ice cores, *J. Geophys. Res.*, **102**(C12), 26,547–26,557.
- Chappellaz, J., T. Blunier, S. Kints, A. Dällenbach, J. M. Barnola, J. Schwander, D. Raynaud, and B. Stauffer (1997b), Changes in the atmospheric CH₄ gradient between Greenland and Antarctica during the Holocene, *J. Geophys. Res.*, **102**(D13), 15,987–15,997.
- Cuffey, K. M., and S. J. Marshall (2000), Substantial contribution to sea-level rise during the last interglacial from the Greenland ice sheet, *Nature*, **404**, 591–594.
- Dansgaard, W., S. J. Johnsen, H. B. Clausen, D. Dahl-Jensen, N. S. Gundestrup, C. U. Hammer, J. P. Steffensen, A. Sveinbjörnsdóttir, J. Jouzel, and G. Bond (1993), Evidence for general instability of past climate from a 250-ky ice-core record, *Nature*, **364**, 218–220.
- Gouzy, A., B. Malaize, C. Pujol, and K. Charlier (2004), Climatic “pause” during Termination II identified in shallow and intermediate waters off the Iberian margin, *Quat. Sci. Rev.*, **23**, 1523–1528.
- GRIP Project Members (1993), Climatic instability during the last interglacial period revealed in the Greenland summit ice core, *Nature*, **364**, 203–207.
- Grootes, P. M., M. Stuiver, J. W.C. White, S. J. Johnsen, and J. Jouzel (1993), Comparison of oxygen isotope records from the GISP2 and GRIP Greenland ice cores, *Nature*, **366**, 552–554.
- Hein, R., P. J. Crutzen, and M. Heimann (1997), An inverse modeling approach to investigate the global atmospheric methane cycle, *Global Biogeochem. Cycles*, **11**, 43–76.
- Herron, M. M., and C. C. Langway Jr. (1980), Firn densification: An empirical model, *J. Glaciol.*, **25**, 373–385.
- Johnsen, S. J., W. Dansgaard, H. B. Clausen, and C. C. Langway Jr. (1972), Oxygen isotope profiles through the Antarctic and Greenland ice sheets, *Nature*, **235**, 429–434.
- Johnsen, S. J., D. Dahl-Jensen, W. Dansgaard, and N. Gundestrup (1995), Greenland palaeotemperatures derived from GRIP bore hole temperature and ice core isotope profiles, *Tellus, Ser. B*, **47**, 624–629.
- Khalil, M. A. K., and R. A. Rasmussen (1983), Sources, sinks, and seasonal cycles of atmospheric methane, *J. Geophys. Res.*, **88**(C9), 5131–5144.
- Krinner, G., D. Raynaud, C. Doutriaux, and H. Dang (2000), Simulations of the Last Glacial Maximum ice sheet surface climate: Implications for the interpretation of ice core air content, *J. Geophys. Res.*, **105**(D2), 2059–2070.
- Landais, A., et al. (2003), A tentative reconstruction of the last interglacial and glacial inception in Greenland based on new gas measurements in the Greenland Ice Core Project (GRIP) ice core, *J. Geophys. Res.*, **108**(D18), 4563, doi:10.1029/2002JD003147.
- Landais, A., J. P. Steffensen, N. Callion, J. Jouzel, V. Masson-Delmotte, and J. Schwander (2004), Evidence for stratigraphic distortion in Greenland Ice Core Project (GRIP) ice core during Event 5e1 (120 kyr BP) from gas isotopes, *J. Geophys. Res.*, **109**, D06103, doi:10.1029/2003JD004193.
- Landais, A., V. Masson-Delmotte, J. Jouzel, D. Raynaud, S. Johnsen, C. Huber, M. Leuenberger, J. Schwander, and B. Minster (2006), The glacial inception recorded in the NorthGRIP Greenland ice core: Timing, structure and associated abrupt temperature changes, *Clim. Dyn.*, in press.
- Lelieveld, J., P. J. Crutzen, and F. J. Dentener (1998), Changing concentration, lifetime and climate forcing of atmospheric methane, *Tellus, Ser. B*, **50**(2), 128–150.
- Luz, B., E. Barkan, M. L. Bender, M. H. Thiemens, and K. A. Boering (1999), Triple-isotope composition of atmospheric oxygen as a tracer of biosphere productivity, *Nature*, **400**, 547–550.
- Mayewski, P. A., L. D. Meeker, M. S. Twickler, S. Whitlow, Q. Yang, W. B. Lyons, and M. Prentice (1997), Major features and forcing of high-latitude northern hemisphere atmospheric circulation using a 110,000-year-long glaciochemical series, *J. Geophys. Res.*, **102**(C12), 26,345–26,366.
- Meese, D. A., et al. (1994), Preliminary depth-agescale of the GISP2 ice core, *Spec. CRREL Rep.* 94-1.
- North Greenland Ice Core Project Members (2004), High-resolution record of Northern Hemisphere climate extending into the last interglacial period, *Nature*, **431**, 147–151.
- Petit, J. R., et al. (1999), Climate and atmospheric history of the past 420,000 years from the Vostok ice core, Antarctica, *Nature*, **399**, 429–436.
- Prinn, R. G., R. F. Weiss, B. R. Miller, J. Huang, F. N. Aleya, D. M. Cunnold, P. J. Fraser, D. E. Hartley, and P. G. Simmonds (1995), Atmospheric trends and lifetime of CH₃CCl₃ and global OH concentrations, *Science*, **269**, 187–192.
- Raynaud, D., J. Chappellaz, C. Ritz, and P. Martinerie (1997), Air content along the Greenland Ice Core Project core: A record of surface climatic parameters and elevation in central Greenland, *J. Geophys. Res.*, **102**(C12), 26,607–26,613.

- Sanchez Goni, M. F., F. Eynaud, J. L. Turon, and N. J. Shackleton (1999), High resolution palynological record off the Iberian margin: Direct land-sea correlation for the Last Interglacial complex, *Earth Planet. Sci. Lett.*, *171*, 123–137.
- Schwander, J., J.-M. Barnola, C. Andrie, M. Leuenberger, A. Ludin, D. Raynaud, and B. Stauffer (1993), The age of the air in the firm and the ice at Summit, Greenland, *J. Geophys. Res.*, *98*(D2), 2831–2838.
- Severinghaus, J. P., and E. J. Brook (1999), Abrupt climate change at the end of the last glacial period inferred from trapped air in polar ice, *Science*, *286*, 930–934.
- Severinghaus, J. P., T. Sowers, E. J. Brook, R. B. Alley, and M. L. Bender (1998), Timing of abrupt climate change at the end of the Younger Dryas interval from thermally fractionated gases in polar ice, *Nature*, *391*, 141–146.
- Severinghaus, J. P., A. Grachev, and M. Battle (2001), Thermal fractionation of air in polar firm by seasonal temperature gradients, *Geochem. Geophys. Geosyst.*, *2*(7), doi:10.1029/2000GC000146.
- Souchez, R., L. Janssens, M. Lemmens, and B. Stauffer (1995), Very low oxygen concentration in basal ice from Summit, Central Greenland, *Geophys. Res. Lett.*, *22*, 2001–2004.
- Sowers, T., M. Bender, and D. Raynaud (1989), Elemental and isotopic composition of occluded O₂ and N₂ in polar ice, *J. Geophys. Res.*, *94*(D4), 5137–5150.
- Sowers, T., M. Bender, L. Labeyrie, D. Martinson, J. Jouzel, D. Raynaud, J. J. Pichon, and Y. S. Korotkevich (1993), A 135,000 year Vostok-SPECMAP common temporal framework, *Paleoceanography*, *8*, 737–766.
- Sowers, T., et al. (1997), An interlaboratory comparison of techniques for extracting and analyzing trapped gases in ice cores, *J. Geophys. Res.*, *102*(C12), 26,527–26,538.
-
- M. L. Bender and M. Suwa, Department of Geosciences, Princeton University, Guyot Hall, Washington Road, Princeton, NJ 08544-1003, USA. (bender@princeton.edu; msuwa@princeton.edu)
- E. J. Brook, Department of Geosciences, Oregon State University, Wilkinson Hall, Corvallis, OR 9731-5506, USA. (brooke@geo.oregonstate.edu)
- A. Landais, Institute of Earth Sciences, Hebrew University of Jerusalem, Jerusalem 91904, Israel. (landais@vms.huji.ac.il)
- J. C. von Fischer, Department of Biology, Colorado State University, Fort Collins, CO 80523, USA. (jcvf@lamar.colostate.edu)